Published in final edited form as:
Toxicol Lett. 2010 July 1; 196(2): 110–116. doi:10.1016/j.toxlet.2010.04.005.

PCB-153 EXPOSURE COORDINATES CELL CYCLE PROGRESSION AND CELLULAR METABOLISM IN HUMAN MAMMARY EPITHELIAL CELLS

Venkatasubbaiah A. Venkatesha, **Amanda L. Kalen**, **Ehab H. Sarsour**, and **Prabhat C. Goswam**
Free Radical and Radiation Biology Program, Department of Radiation Oncology, The University of Iowa, Iowa City, Iowa, USA

Abstract

2,2',4,4',5,5'-hexachlorobiphenyl (PCB-153) is a non-metabolizable environmental chemical contaminant commonly found in breast milk of PCB exposed individuals, suggesting that chronic exposure to PCB-153 could have adverse health effects. We have shown previously that PCB-153 increased reactive oxygen species levels in non-tumorigenic MCF-10A human mammary epithelial cells, which were associated with DNA damage, growth inhibition, and cytotoxicity. This study investigates the hypothesis that PCB-153 exposure coordinates cell cycle progression and cellular metabolism by inhibiting cyclin D1 accumulation. PCB-153 treated MCF-10A cells exhibited a dose and time dependent decrease in cyclin D1 protein levels. The decrease in cyclin D1 protein levels was associated with an inhibition in AKT and GSK-3β phosphorylation, which correlated with an increase in cyclin D1-T286 phosphorylation. Fibroblasts carrying a mutant form of cyclin D1 (T286A) were resistant to PCB-153 induced degradation of cyclin D1. Pre-treatment of cells with a proteasome inhibitor (MG132) suppressed PCB-153 induced decrease in cyclin D1 protein levels. Interestingly, suppression in cyclin D1 accumulation was associated with an increase in cellular glucose consumption, and hexokinase II and pyruvate kinase protein levels. These results suggest that cyclin D1 coordinates cell cycle progression and cellular metabolism in PCB-153 treated non-tumorigenic human mammary epithelial cells.

Keywords

PCB-153; epithelial cells; cyclin D1; AKT; hexokinase; pyruvate kinase; cell cycle; glucose

1. INTRODUCTION

Polychlorinated biphenyls (PCBs) were produced in the United States over a 50-year period as Aroclors. PCBs were found to have adverse biological effects in humans and animals, and their production was banned in the United States in 1977. PCBs are persistent environmental contaminants because of their intensive industrial uses, and improper disposal practices.

Address for correspondence to: Prabhat C. Goswami, Ph.D, Free Radical and Radiation Biology Program, Department of Radiation Oncology, The University of Iowa, 500 Newton Road, Iowa City, IA 52242-1181. Phone: 319-335-8019; Fax: 319-335-8039 prabhat-goswami@uiowa.edu .

PCB-153 (2,2',4,4',5,5'-hexachlorobiphenyl) is a non-coplanar ortho- and para-substituted non-dioxin like PCB, which is present in aroclors 1248, 1254, and 1260. Thus, PCB-153 is one of the most common PCB contaminants in nature. PCB-153 is detected in human serum, adipose tissue, breast milk, dairy products, vegetable oil, and fish (Park et al., 2009; Radice et al., 2008; Wang et al., 2008). The biological half-life of PCB-153 is reported to be 110 years, which makes it a long-lived environmental contaminant with potentials for adverse biological effects (Jonsson et al., 2003).

Exposure to PCB-153 has been reported to cause a wide array of biological effects, such as perturbations of endocrine functions and sex hormone synthesis, reproductive defects, DNA damage, nephro-, immuno- and lung-toxicities (Chen et al., 2006; Craft et al., 2002; Johansson et al., 2006; Jung et al., 2005; Lyche et al., 2006; Oskam et al., 2005; Sipka et al., 2008; Venkatesha et al., 2008). Furthermore, the evidence for liver toxicity, tumor promotion, and oral squamous cell carcinoma formation suggests that PCB-153 exposures could perturb cellular proliferation (Glauert et al., 2008; Strathmann et al., 2006; Yoshizawa et al., 2005).

Cellular proliferation is a tightly regulated sequence of progression from G_0/G_1 to S to G_2 and M that requires the activation of specific cyclin dependent kinases (CDKs) and simultaneous inhibition of CDK inhibitors (Grana and Reddy, 1995). The progression from G_0/G_1 to S in response to mitogenic stimuli is regulated by the accumulation and assembly of D-type cyclins with CDK4/6 (Alt et al., 2000). Cyclin A and B in association with CDK2 and CDK1 regulate progression through S, G_2 and M. PCB-153 treatments are known to decrease hepatic mRNA levels of cyclin A, B1, and B2 in mice (Lu et al., 2004).

Cyclin D1 is a nuclear localized protein that regulates nuclear processes during progression from G_1 to S. Recent reports by Sakamaki *et al.*, and Wang *et al.* demonstrate that cyclin D1/CDK4/6 activity also regulates cellular metabolism (Sakamaki et al., 2006; Wang et al., 2006). Physiological levels of cyclin D1 decrease aerobic glycolysis, mitochondrial function, and mitochondria size *in vivo*. Mitochondrial functions are enhanced by genetic deletion of cyclin D1 (Sakamaki et al., 2006). Cyclin D1 phosphorylates the transcription factor nuclear respiratory factor 1 (NRF1) at ser-47; phosphorylated NRF1 suppresses the expression of nuclear encoded mitochondrial genes (Wang et al., 2006). Dephosphorylation of NRF1 in the absence of cyclin D1 promotes its transcriptional activity which enhances the expression of nuclear encoded mitochondria genes, including hexokinase II and pyruvate kinase.

In this study, we investigate the hypothesis that cyclin D1 coordinates cell cycle progression with cellular metabolism in PCB-153 treated MCF-10A non-tumorigenic human mammary epithelial cells. Our results show PCB-153 induced inhibition in cell cycle progression was associated with a significant decrease in cyclin D1 protein levels and enhanced glucose consumption.

2. MATERIALS AND METHODS

2.1. Cell culture

MCF-10A human non-tumorigenic mammary epithelial cells were purchased from the American Tissue Culture Collection. MCF-10A cells are immortalized diploid cells that possess normal epithelial characteristics. Cells were cultured following our previously published protocol (Venkatesha et al., 2008). NIH3T3 and NIH3T3-Flag D1-T286A mouse fibroblasts were gifts from Dr. Alan Diehl, University of Pennsylvania. Monolayer cultures were maintained in DMEM (Gibco) supplemented with 10 % FBS, 1 × glutamine, antibiotics (100 units/ml penicillin and 100 μg/ml streptomycin). NIH3T3-Flag D1-T286A fibroblasts were cultured in medium containing puromycin (BD Biosciences). N-[(Phenylmethoxy)

carbonyl]-L-leucyl-N-[(1S)-1-formyl-3-methylbutyl]-L-leucinamide (MG132), was purchased from the Sigma Chemical Company.

2.2. PCB congeners

PCB congeners, 2,2′,4,4′,5,5′-hexachlorobiphenyl (PCB-153) and 4-chloro biphenyl (PCB-3) were provided by Dr. Hans J. Lehmler in the Occupational & Environmental Health Center at the University of Iowa. The compounds were synthesized and characterized as described previously (Amaro et al., 1996; Schramm et al., 1985). PCB stock solutions were prepared using dimethyl sulfoxide; the final concentration of DMSO in culture medium was kept below 0.5%. Cell growth was determined by counting cells in a Z1 Coulter Counter, Beckman Coulter.

2.3. Flow cytometry assay

Cell cycle phase distributions were analyzed by flow cytometry measurements of DNA content following our previously published protocol (Menon et al., 2003; Venkatesha et al., 2008). Briefly, ethanol-fixed cells were washed with DPBS and incubated with RNase A and propidium iodide (35 μg ml^{-1}). PI fluorescence was measured by flow cytometry (BD FACScan); data were collected from 10,000 cells in list mode, and cell cycle phase distributions calculated using MODFIT software (Verity Software House).

2.4. Immunoblotting assay

Equal amounts of total cellular protein extracts were separated on 15% SDS-PAGE and electro-blotted onto a nitrocellulose membrane. The membrane was incubated with TBST buffer containing 5% nonfat dry milk (0.1 M Tris-HCl, pH 7.5, 0.15 M NaCl and 0.1% Tween-20). Blots were incubated with primary antibodies to cyclin D1 (1:1500; DCS-6 mouse monoclonal, BD Pharmingen), Cdk6 (1:1000 polyclonal rabbit antiserum, BD Pharmingen), cyclin A (1:1000; C-19, rabbit polyclonal, Santa Cruz Biotechnology), phospho-Thr286 cyclin D1 (1:1000; 2921 rabbit polyclonal, Cell Signaling), pyruvate kinase (1:5000; rabbit polyclonal, Rockland Immunochemicals), hexokinase II (1:1000; C64G5 rabbit monoclonal, Cell Signaling), phospho-GSK-3β (Ser 21/9, 1:1000; rabbit polyclonal, Cell Signaling), and phospho-AKT (Ser473, 1:1000; rabbit polyclonal, Cell Signaling). Immunoreactive bands were visualized by an enhanced chemiluminescence kit (GE Healthcare). Actin and tubulin levels were used for comparison. Results were quantitated using Image J software (NIH) and calculated relative to actin levels in individual samples.

In proteasome inhibition experiment, MG132 was added 45 min prior to the PCB-153 treatment, and total protein extracts were prepared 4 h later for cyclin D1 immunoblotting assay.

2.5. Quantitative RT-PCR assay

One microgram of total RNA was reverse transcribed using random-hexamer primers and reverse transcriptase. PCR primers for cyclin D1 and 18S were as follows: cyclin D1, forward primer: 5’-AGAAGCTGTGCATCTACACCGACAA-3’, reverse primer: 5’-GGCATTTTGGAGAGGAAGTGTTCAA-3’, amplicon size 142 bp; 18S, forward primer: 5’-CCTTGGATGTGGTAGCCGTTT-3’, reverse primer: 5’-AACTTTCGATGGTAGTCGCCG-3’, amplicon size 105 bp. PCR assay was performed using POWER-SYBR Green PCR Mastermix (Applied Biosystems), 2 μl of cDNA, and 5 μM of primers. The PCR amplification was done in an ABI 7000 thermal cycler using the absolute quantification method; cycle parameters were 95°C for 10 min followed by 40 cycles of 15 sec at 95°C and 1 min at 60°C. Cycle threshold (Ct) was calculated from each sample with the ABI Prism 7000 Sequence Detection Software. Relative mRNA levels of cyclin D1 was

calculated using the formulas: $\Delta Ct = Ct$ (cyclin D1) − Ct (18S); $\Delta\Delta Ct = \Delta Ct$ (treatment) – ΔCt (control); and Expression = $2^{-\Delta\Delta Ct}$.

2.6. Glucose consumption assay

MCF-10A monolayer cultures were treated with PCB-153 for 8 h. The culture medium containing PCB-153 was removed; washed the monolayer cells with pre-equilibrated Dulbecco's phosphate buffered saline followed by incubation in fresh pre-equilibrated medium containing PCB-153 for an additional 8 h. Media samples were collected at the time of addition of the fresh medium and 8 h post-addition. The glucose content in media samples were measured using Accu-Chek Aviva (Strips code 951, Cat # 04538412001, Roche). The glucose content from the untreated and treated groups were normalized to the cell count and expressed as picomoles glucose consumed/cell for the duration of the PCB-153 treatment. The reliability of strip based glucose estimations was shown to be completely consistent with the standard colorimetric assay (Nayak and Herman, 1997).

2.7 Statistical Analysis

Statistical significance was determined by ANOVA with Tukey's honesty *post hoc* test for test groups more than three or paired student 't' test for less than 3 test groups; 95% confidence interval was applied. Results are presented as mean ± standard deviation. Data with $p < 0.05$ were considered significant. Statistical analysis was done using SPSS statistical package software, version 17 (SPSS Inc., Chicago, IL).

3. RESULTS

3.1. PCB-153 treatment inhibits entry into S-phase

To determine if exposure to PCB-153 perturbs cellular proliferation, MCF-10A non-tumorigenic human mammary epithelial cultures were incubated with PCB-153 (0–15 μM) for 4, 24, and 48 h and assayed for cell cycle phase distributions by measuring DNA content. Representative DNA histograms are shown in Figure 1B and the percentages of G_1 and S +G_2+M cells are presented in Figure 1 C&D. PCB-153 treatment for 4 h did not show any significant change in cell cycle phase distributions compared to DMSO-treated control. At 24 and 48 h post-treatment, the percentage of G_1 cells in controls decreased to approximately 70% coinciding with an increase (approximately 30%) in the percentage of S+G_2+M cells, indicating that the control cells were progressing through the cell cycle. However, the percentage of G_1 in PCB-153 treated cells remained high (90–95%) coinciding with a significant inhibition in the percentage of S+G_2+M cells at 24 and 48 h post-treatment. These results showed that PCB-153 treatments inhibited entry into S-phase.

3.2 PCB-153 treatments decreased cyclin D1 expression

Cell cycle progression from G_1 to S-phase is primarily controlled by the D-type cyclins in association with CDK4/6. To determine if the PCB-153 induced inhibition in entry into S-phase is due to a change in cyclin D1 expression, MCF-10A cells were incubated with PCB-153 (0–15 μM) for 4 h. Total cellular protein extracts were analyzed for cyclin D1 protein levels by immunoblotting (Figure 2). PCB-153 treatments resulted in a dose-dependent decrease in cyclin D1 protein levels; approximately 50% decrease in 5 μM treated cells, and more than 95% decrease in 10 and 15 μM treated cells (Figure 2A&C). PCB-153 treatments did not affect CDK6 and cyclin A protein levels, suggesting the specificity of this effect to cyclin D1 (Figure 2A). Interestingly, similar treatments with PCB-3 (4-monochloro biphenyl) did not show any change in cyclin D1 protein levels (Figure 2B).

To determine if the decrease in cyclin D1 protein levels in PCB-153 treated cells could be due to a decrease in cyclin D1 mRNA levels, a quantitative RT-PCR assay was applied (Figure 2D). Cyclin D1 mRNA levels in 3 and 5 μM PCB-153-treated cells were not significantly different compared to untreated controls. However, cyclin D1 mRNA levels were reduced to 50% in 10 μM PCB-153 treated cells, and less than 20% cyclin D1 mRNA remained in 15 μM PCB-153 treated cells. These results suggest that lower doses of PCB-153 could activate cyclin D1 protein turnover, while higher doses could inhibit cyclin D1 transcription as well as enhance cyclin D1 protein degradation.

3.3. A dose and time dependent decrease in cyclin D1 protein levels in PCB-153 treated cells

To determine the optimal conditions for the effect of PCB-153 on cyclin D1 protein levels, MCF-10A cells were treated with 0–10 μM PCB-153 for 0–8 h (Figure 3). Cyclin D1 protein levels significantly decreased in 3 μM PCB-153 treated cells, approximately 50% at 8 h post-treatment. Cyclin D1 protein levels in 5 μM PCB-153 treated cells decreased approximately 50% at 2 h post-treatment and remained low until 8 h post-treatment. Higher dose of PCB-153 (10 μM) resulted in a significant decrease (approximately 75%) in cyclin D1 protein levels at 4 h post-treatment, which continued to decrease (more than 90%) at 8 h post-treatment. These results suggest lower doses of PCB-153 could elicit a transient response, while higher doses could have a long term effect on cyclin D1 protein levels.

3.4. PCB-153 induces phosphorylation-dependent proteasomal degradation of cyclin D1 protein

To determine if a proteasomal degradation pathway could regulate cyclin D1 protein levels in PCB-153 treated cells, MCF-10A cells were incubated with a proteasome inhibitor, MG132, prior to the addition of PCB-153. Cyclin D1 protein levels were analyzed by immunoblotting at the end of 4 h of PCB-153 treatment (Figure 4A). As anticipated MG132 pre-treatment stabilized cyclin D1 in control cells; approximately 1.8-fold increase (lane 2) compared to untreated control (lane 1, $p < 0.05$). Consistent with the results presented in Figures 2 and 3, PCB-153 treatments significantly decreased (0.6-fold) cyclin D1 protein levels (Figure 4A, lanes 3 and 5 compared to lane 1, $p < 0.05$). However, prior treatments with MG132 significantly inhibited PCB-153 induced degradation of cyclin D1 protein levels (compare lanes 4 and 6 to lanes 3 and 5).

Phosphorylation at threonine 286 is known to degrade cyclin D1. To determine if the PCB-153 induced degradation in cyclin D1 could be mediated via the T286 phosphorylation pathway, NIH3T3 mouse fibroblasts expressing either wild type or T286A mutant form of cyclin D1 were incubated with 10 μM PCB-153 for 4 h and immunoblotted for cyclin D1 protein levels. PCB-153 treatment significantly decreased (70%) cyclin D1 protein levels in NIH3T3 wild type fibroblasts (Figure 4B, compare lane 2 *vs*. lane 1; $p<0.05$). As expected, cyclin D1 basal level in the mutant cell line was higher compared to wild type cells (Figure 4B, compare lane 3 *vs*. lane 1). However, PCB-153 treatment did not show any change in cyclin D1 protein levels in NIH3T3 fibroblasts carrying the T286A mutant form of cyclin D1 (Figure 4B, compare lane 4 *vs*. lane 3). T286-dependent degradation of cyclin D1 in PCB-153 treated MCF-10A cells were further evaluated by immunoblotting using an antibody specific for the T286 phosphorylation site (Figure 4B, lower panel). Results showed PCB-153 treatment of MCF-10A cells increased the T286-phosphorylated form of cyclin D1. These results suggest that PCB-153 induced degradation of cyclin D1 could be mediated via the T286-phosphorylation pathway.

GSK-3β is known to phosphorylate T286 of cyclin D1 promoting its nuclear export and polyubiquitination followed by 26S proteasome-mediated degradation (Diehl et al., 1998; Diehl et al., 1997). GSK-3β is a substrate for AKT; phosphorylated GSK-3β is kinase inactive

(Delcommenne et al., 1998). To determine if PCB-153 induced degradation of cyclin D1 is associated with changes in the phosphorylation status of GSK-3β and AKT, MCF-10A cells were incubated with PCB-153 (0–10 μM) for 4 h and immunoblotted for the measurements of cyclin D1, phosphorylated GSK-3β and AKT protein levels (Figure 4C). Similar to the results presented in Figures 2 & 3, PCB-153 treatments showed a dose-dependent decrease in cyclin D1 protein levels. PCB-153 treatments inhibited AKT and GSK-3β phosphorylation. While phosphorylation of AKT inhibits its kinase activity, inhibition of GSK-3β phosphorylation activates its kinase activity (Delcommenne et al., 1998). Hypophosphorylated GSK-3β is anticipated to phosphorylate cyclin D1 (T286) targeting it for degradation.

3.5. Cyclin D1 coordinates cell cycle progression and cellular metabolism in PCB-153 treated cells

To determine if cyclin D1 degradation influences glycolysis, glucose consumption was measured in control and PCB-153 treated cells (Figure 5A). Glucose consumption in control cells was measured to be 33 picomoles/cell. Interestingly, PCB-153 treatments increased glucose consumption 1.5–3 folds (Figure 5A). The increase in glucose consumption inversely correlated with cyclin D1 protein levels, suggesting that cyclin D1 could coordinate glycolysis and cell proliferation in PCB-153 treated MCF-10A cells.

Immunoblotting assays were performed to determine if PCB-153 induced increase in glucose consumptions were associated with changes in glycolytic enzymes, hexokinase II (converts glucose to glucose 6-phosphate) and pyruvate kinase (converts phosphoenol pyruvate to pyruvate). The protein levels of hexokinase II and pyruvate kinase increased approximately 1.8 fold in 1 μM PCB-153 treated MCF-10A cells compared to untreated controls (Figure 5B). The higher doses of PCB-153 treatments showed approximately 3-fold increase in hexokinase II, and 2-fold increase in pyruvate kinase protein levels.

4. DISCUSSION

The present study investigates the hypothesis that PCB-153 exposure coordinates cell cycle progression and cellular metabolism by inhibiting cyclin D1 accumulation. Cyclin D1 is the first cell cycle regulatory protein that responds to mitogenic stimuli (Alt et al., 2000). PCB-153 showed a dose dependent decrease in cyclin D1 protein levels that was consistent with a corresponding inhibition in cells' entry into S-phase (Figures 1&2). These results were specific to the PCB-153 treatments because a similar treatment with PCB-3 did not show any change in cyclin D1 protein levels (Figure 2B). The decrease in cyclin D1 protein levels was observed as early as 2 h of PCB-153 treatments (Figure 3), suggesting that a decrease in cyclin D1 protein levels could lead to an inhibition in entry into S-phase rather than cell cycle redistributions to G_1-phase leading to the degradation of cyclin D1 (Figure 1). PCB-153 treatments did not show any change in CDK6 and cyclin A protein levels (Figure 2A) indicating that PCB-153 could specifically interfere with the mitogenic response of cyclin D1 during progression from G_1 to S phase.

A previous study showed a very small decrease (<5%) in cyclin A2, B1, B2, and C mRNA levels in liver tissues of eight-weeks-old B6.129 mice that were treated with PCB-153 for 2 d (Lu et al., 2004). The authors did not show if such a small change in mRNA levels resulted in any change in the corresponding protein levels. The same treatment did not cause any change in cyclin D1 mRNA and protein levels. While PCB-153 treatments decreased cyclin A2, B1, B2, and C mRNA levels, it is puzzling how these treatments could enhance cell proliferation (Lu et al., 2004). One possible explanation could be that the increase in cell proliferation was in response to PCB-153 induced cell loss. Our results show a dose and time dependent decrease in cyclin D1 protein levels. While the lower doses of PCB-153 degrade cyclin D1 protein, higher doses of PCB-153 decreased cyclin D1 mRNA (Figure 2). These results suggest

PCB-153 exposure can negatively impact upon cyclin D1 protein and mRNA levels. The difference in results of increased proliferation in hepatocytes of PCB-153 exposed mice (Lu et al., 2004) compared to inhibition in proliferation of human mammary epithelial cells in our study could be due to the difference in dose and duration of the PCB-153 exposures and cell type difference, mouse hepatocytes vs. human mammary epithelial cells. Alternatively, these differences could also be due to a difference in cellular microenvironment and oxygen concentrations 21% oxygen in *in vitro* cell culture experiments compared to approximately 4% oxygen concentration *in vivo*.

GSK-3β is known to phosphorylate T286 of cyclin D1 targeting it for proteasome-mediated degradation (Diehl et al., 1998). GSK-3β is phosphorylated by AKT. Phosphorylated GSK-3β is kinase inactive, while the unphosphorylated form confers its kinase activity. The kinase activity of AKT is governed by its phosphorylated form (Delcommenne et al., 1998; Ushio-Fukai et al., 1999). The phosphorylation status of AKT and GSK-3β are most commonly used as indicators of their kinase activities. Thus, a decrease in AKT phosphorylation is anticipated to decrease phosphorylation of GSK-3β, which is expected to enhance the kinase activity of GSK-3β. An active GSK-3β is expected to phosphorylate T286 of cyclin D1 and target it for degradation. Indeed this is what we found in results presented in Figure 4. PCB-153 treatments inhibited phosphorylation of both AKT and GSK-3β. Considering hypophosphorylated GSK-3β being kinase-active and cyclin D1 (T286) is a substrate for GSK-3β, it is anticipated that PCB-153 induced activation of GSK-3β kinase would increase cyclin D1 T286 phosphorylation. Results from the immunoblotting assay using antibodies specific to the T286-phosphorylated form of cyclin D1 showed a significant increase in T286-phosphorylation in 3–10 μM PCB-153 treated MCF-10A cells (Figure 4B, bottom panel). PCB-153 induced T286 phosphorylation of cyclin D1 was also evident from results presented in Figure 4B (upper panel). These results show that the PCB-153 treatments failed to degrade cyclin D1 in NIH3T3 fibroblasts harboring the mutant form of cyclin D1 (T286A). These results clearly indicate that phosphorylation at the T286-site regulates cyclin D1 degradation in PCB-153 treated MCF-10A cells.

A previous report by Sakamaki *et al.* demonstrates a negative correlation between cyclin D1 protein levels and cellular metabolism (Sakamaki et al., 2006). Aerobic glycolysis, mitochondrial function, and mitochondria size decreased *in vivo* in presence of physiological levels of cyclin D1. In contrast deletion of cyclin D1 increased glycolysis, which corresponds to an increase in the expression of hexokinase II and pyruvate kinase (Sakamaki et al., 2006). Consistent with these previous observations, an inverse correlation was observed between cyclin D1 protein levels and glucose consumption in PCB-153 treated MCF-10A cells (Figure 5A). The increase in glucose consumption in PCB-153 treated cells was also associated with an increase in hexokinase II and pyruvate kinase protein levels (Figure 5B). An earlier report by Wang *et al.* (Wang et al., 2006) showed that cyclin D1-dependent phosphorylation of NRF1 transcription factor inhibited the expression of nuclear encoded mitochondrial genes (Wang et al., 2006). Dephosphorylation of NRF1 in the absence of cyclin D1 enhanced its transcriptional activity, which subsequently enhanced the expression of glycolytic genes including the expression of hexokinase II and pyruvate kinase. Additional experiments are necessary to determine if a similar pathway regulates the activation of hexokinase II and pyruvate kinase expression in PCB-153 treated MCF-10A cells.

In summary, PCB-153 induced decrease in cyclin D1 was accompanied with an increase in hexokinase II and pyruvate kinase protein levels, which was associated with an increase in the rate of glucose consumption. We believe these results are the first report of cyclin D1 regulating cell cycle progression and cellular metabolism in PCB-153 exposed non-tumorigenic human mammary epithelial cells. The significance of our results could be applicable to the possible impairment of cell and tissue regeneration in PCB exposed individuals.

Acknowledgments

We thank Drs. Larry W. Robertson and Hans J. Lehmler at the Occupational & Environmental Health for providing us with the PCBs, the staff at the Flow Cytometry Core Facility, Dr. J. Alan Diehl (University of Pennsylvania) for NIH3T3 Flag-cyclin D1-T286A cell line. Funding from NIEHS (P42 ES 013661) and NIH (CA 111365) supported this work.

ABBREVIATIONS

PCB-153	2,2',4,4',5,5'-hexachlorobiphenyl
PCB-126	3,3',4,4',5-pentachlorobiphenyl
PCB-3	4-monochloro biphenyl
DMSO	dimethyl sulfoxide
RT-PCR	reverse transcriptase polymerase chain reaction
AKT	protein kinase B
GSK-3β	glycogen synthase kinase 3β

REFERENCES

Alt JR, Cleveland JL, Hannink M, Diehl JA. Phosphorylation-dependent regulation of cyclin D1 nuclear export and cyclin D1-dependent cellular transformation. Genes & Dev 2000;14:3102–3114. [PubMed: 11124803]

Amaro AR, Oakley GG, Bauer U, Spielmann HP, Robertson LW. Metabolic activation of PCBs to quinones: reactivity toward nitrogen and sulfur nucleophiles and influence of superoxide dismutase. Chem. Res. Toxicol 1996;9:623–629. [PubMed: 8728508]

Chen YQ, De S, Ghosh S, Dutta SK. Congener-specific polychlorinated biphenyl-induced cell death in human kidney cells in vitro: Potential role of caspase. Int. J. Toxicol 2006;25:341–347. [PubMed: 16940006]

Craft ES, DeVito MJ, Crofton KM. Comparative responsiveness of hypothyroxinemia and hepatic enzyme induction in long-evans rats versus C57BL/6J mice exposed to TCDD-like and phenobarbital-like polychlorinated biphenyl congeners. Toxicol. Sci 2002;68:372–380. [PubMed: 12151633]

Delcommenne M, Tan C, Gray V, Rue L, Woodgett J, Dedhar S. Phosphoinositide-3-OH kinase-dependent regulation of glycogen synthase kinase 3 and protein kinase B/AKT by the integrin-linked kinase. Proc. Natl. Acad. Sci., U.S.A 1998;95:11211–11216. [PubMed: 9736715]

Diehl JA, Cheng M, Roussel MF, Sherr CJ. Glycogen synthase kinase-3beta regulates cyclin D1 proteolysis and subcellular localization. Genes & Dev 1998;12:3499–3511. [PubMed: 9832503]

Diehl JA, Zindy F, Sherr CJ. Inhibition of cyclin D1 phosphorylation on threonine-286 prevents its rapid degradation via the ubiquitin-proteasome pathway. Genes & Dev 1997;11:957–972. [PubMed: 9136925]

Glauert HP, Tharappel JC, Banerjee S, Chan NLS, Kania-Korwel I, Lehmler HJ, Lee EY, Robertson LW, Spear BT. Inhibition of the promotion of hepatocarcinogenesis by 2,2 ',4,4 ',5,5 '-hexachlorobiphenyl (PCB-153) by the deletion of the p50 subunit of NF-kappa B in mice. Toxicol. Appl. Pharmacol 2008;232:302–308. [PubMed: 18644402]

Grana X, Reddy EP. Cell Cycle Control in mammalian cells: role of cyclins, cell cycle dependent kinases (CDKs), growth suppressor genes, and cyclin dependent kinase inhibitors (CKIs). Oncogene 1995;11:211–219. [PubMed: 7624138]

Johansson C, Tofighi R, Tamm C, Goldoni M, Mutti A, Ceccatelli S. Cell death mechanisms in AtT20 pituitary cells exposed to polychlorinated biphenyls (PCB 126 and PCB 153) and methylmercury. Toxicol. Lett 2006:183–190. [PubMed: 17049763]

Jonsson A, Gustafsson O, Axelman J, Sundberg H. Global accounting of PCBs in the continental shelf sediments. Environ. Sci. Technol 2003;37:245–245. [PubMed: 12564894]

Jung JH, Jeon JK, Shim WJ, Oh JR, Lee JY, Kim BK, Han CH. Molecular cloning of vitellogenin cDNA in rockfish (Sebastes schlegeli) and effects of 2,2 ' 4,4 ' 5,5 '-hexachlorobiphenyl (PCB 153) on its gene expression. Mar. Pollut. Bull 2005;51:794–800. [PubMed: 16291191]

Lu ZJ, Lee EY, Robertson LW, Glauert HP, Spear BT. Effect of 2,2 ',4,4 ',5,5 '-hexachlorobiphenyl (PCB-153) on hepatocyte proliferation and apoptosis in mice deficient in the p50 subunit of the transcription factor NF-kappa B. Toxicol. Sci 2004;81:35–42. [PubMed: 15201435]

Lyche JL, Larsen HJS, Skaare JU, Tverdal A, Johansen GM, Ropstad E. Perinatal exposure to low doses of PCB 153 and PCB 126 affects maternal and neonatal immunity in goat kids. J. Toxicol. Environ. Health-Part A-Curr. Issues 2006;69:139–158.

Menon SG, Sarsour EH, Spitz DR, Higashikubo R, Sturm M, Zhang H, Goswami PC. Redox regulation of the G1 to S phase transition in the mouse embryo fibroblast cell cycle. Can. Res 2003;63:2109–2117.

Nayak RC, Herman IM. Measurement of glucose consumption by hybridoma cells growing in hollow fiber cartridge bioreactors: use of blood glucose self-monitoring devices. J. Immunol. Meth 1997;205:109–114.

Oskam IC, Lyche JL, Krogenaes A, Thomassen R, Skaare JU, Wiger R, Dahl E, Sweeney T, Stien A, Ropstad E. Effects of long-term maternal exposure to low doses of PCB126 and PCB-153 on the reproductive system and related hormones of young male goats. Reproduction 2005;130:731–742. [PubMed: 16264102]

Park H, Ikonomou MG, Kim HS, Choi JW, Chang YS. Dioxin and dioxin-like PCB profiles in the serum of industrial and municipal waste incinerator workers in Korea. Environ. Int 2009;35:580–587. [PubMed: 19058852]

Radice S, Chiesara E, Fucile S, Marabini L. Different effects of PCB101, PCB118, PCB138 and PCB-153 alone or mixed in MCF-7 breast cancer cells. Food Chem. Toxicol 2008;46:2561–2567. [PubMed: 18508174]

Sakamaki T, Casimiro MC, Ju X, Quong AA, Katiyar S, Liu M, Jiao X, Li A, Zhang X, Lu Y, Wang C, Byers S, Nicholson R, Link T, Shemluck M, Yang J, Fricke ST, Novikoff PM, Papanikolaou A, Arnold A, Albanese C, Pestell R. Cyclin D1 determines mitochondrial function in vivo. Mol. Cell. Biol 2006;26:5449–5469. [PubMed: 16809779]

Schramm H, Robertson LW, Oesch F. Differential regulation of hepatic glutathione transferase and glutathione peroxidase activities in the rat. Biochem. Pharmacol 1985;34:3735–3739. [PubMed: 4052112]

Sipka S, Eum SY, Son KW, Xu S, Gavalas VG, Hennig B, Toborek M. Oral administration of PCBs induces proinflammatory and prometastatic responses. Environ. Toxicol. Pharmacol 2008;25:251–259. [PubMed: 18438459]

Strathmann J, Schwarz M, Tharappel JC, Glauert HP, Spear BT, Robertson LW, Appel KE, Buchmann A. PCB 153, a non-dioxin-like tumor promoter, selects for beta-catenin (Catnb)-mutated mouse liver tumors. Toxicol. Sci 2006;93:34–40. [PubMed: 16782779]

Ushio-Fukai M, Alexander RW, Akers M, Yin Q, Fujio Y, Walsh K, Griendling KK. Reactive oxygen species mediate the activation of Akt/protein kinase B by angiotensin II in vascular smooth muscle cells. J. Biol. Chem 1999;274:22699–22704. [PubMed: 10428852]

Venkatesha VA, Venkataraman S, Sarsour EH, Kalen AL, Buettner GR, Robertson LW, Lehmler HJ, Goswami PC. Catalase ameliorates polychlorinated biphenyl-induced cytotoxicity in nonmalignant human breast epithelial cells. Free Radic. Biol. Med 2008;45:1094–1102. [PubMed: 18691649]

Wang C, Li Z, Lu Y, Du R, Katiyar S, Yang J, Fu M, Leader JE, Quong A, Novikoff PM, Pestell RG. Cyclin D1 repression of nuclear respiratory factor 1 integrates nuclear DNA synthesis and mitochondrial function. Proc. Natl. Acad. Sci., U.S.A 2006;103:11567–11572. [PubMed: 16864783]

Wang YF, Wang SL, Chen FA, Chao HA, Tsou TC, Shy CG, Papke O, Kuo YM, Chao HR. Associations of polybrominated diphenyl ethers (PBDEs) in breast milk and dietary habits and demographic factors in Taiwan. Food Chem. Toxicol 2008;46:1925–1932. [PubMed: 18321630]

Yoshizawa K, Walker NJ, Jokinen MP, Brix AE, Sells DM, Marsh T, Wyde ME, Orzech D, Haseman JK, Nyska A. Gingival carcinogenicity in female Harlan Sprague-Dawley rats following two-year oral treatment with 2,3,7,8-tetrachlorodibenzo-p-dioxin and dioxin-like compounds. Toxicol. Sci 2005;83:64–77. [PubMed: 15509667]

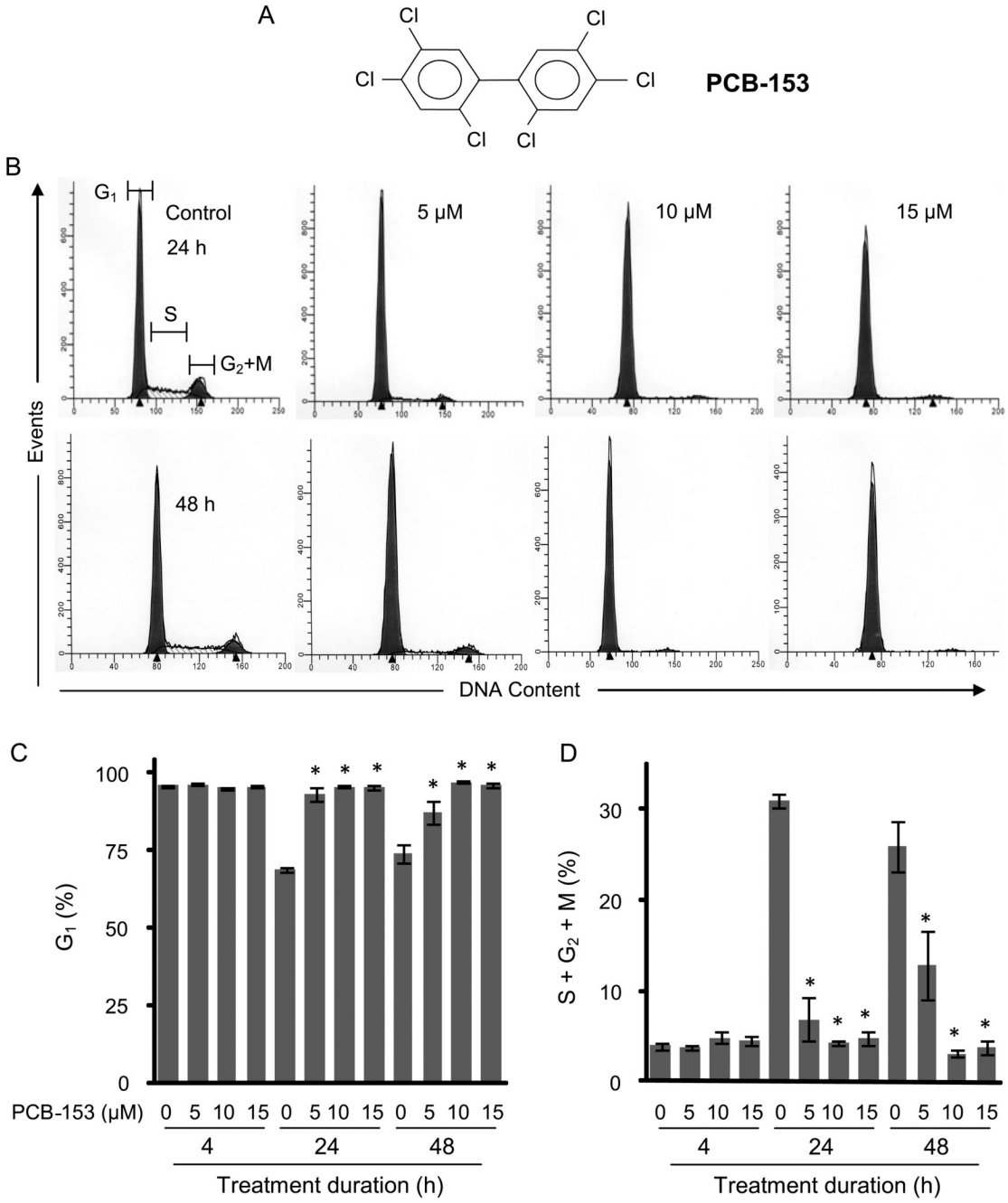

Fig. 1. PCB-153 treatments inhibited entry into S-phase

MCF-10A non-tumorigenic human mammary epithelial cells were incubated with PCB-153 for the indicated times. Cells were harvested for flow cytometry measurements of DNA content. **(A)** Chemical structure of PCB-153 (2,2',4,4',5,5'-hexachlorobiphenyl); **(B)** Representative DNA histograms at the end of 4, 24 and 48 h of PCB-153 treatments; the percentages of G_1 **(C)** and $S+G_2+M$ **(D)** were calculated using Cell-Quest software. The percentage of cells in G_1 and $S+G_2+M$ phases is expressed as the mean of three independent experiments run in duplicate. ANOVA followed by Tukey's *post hoc* test were used to assess statistical significance of results. Asterisks represent significant difference between control and treated samples ($n=3$, $p < 0.05$).

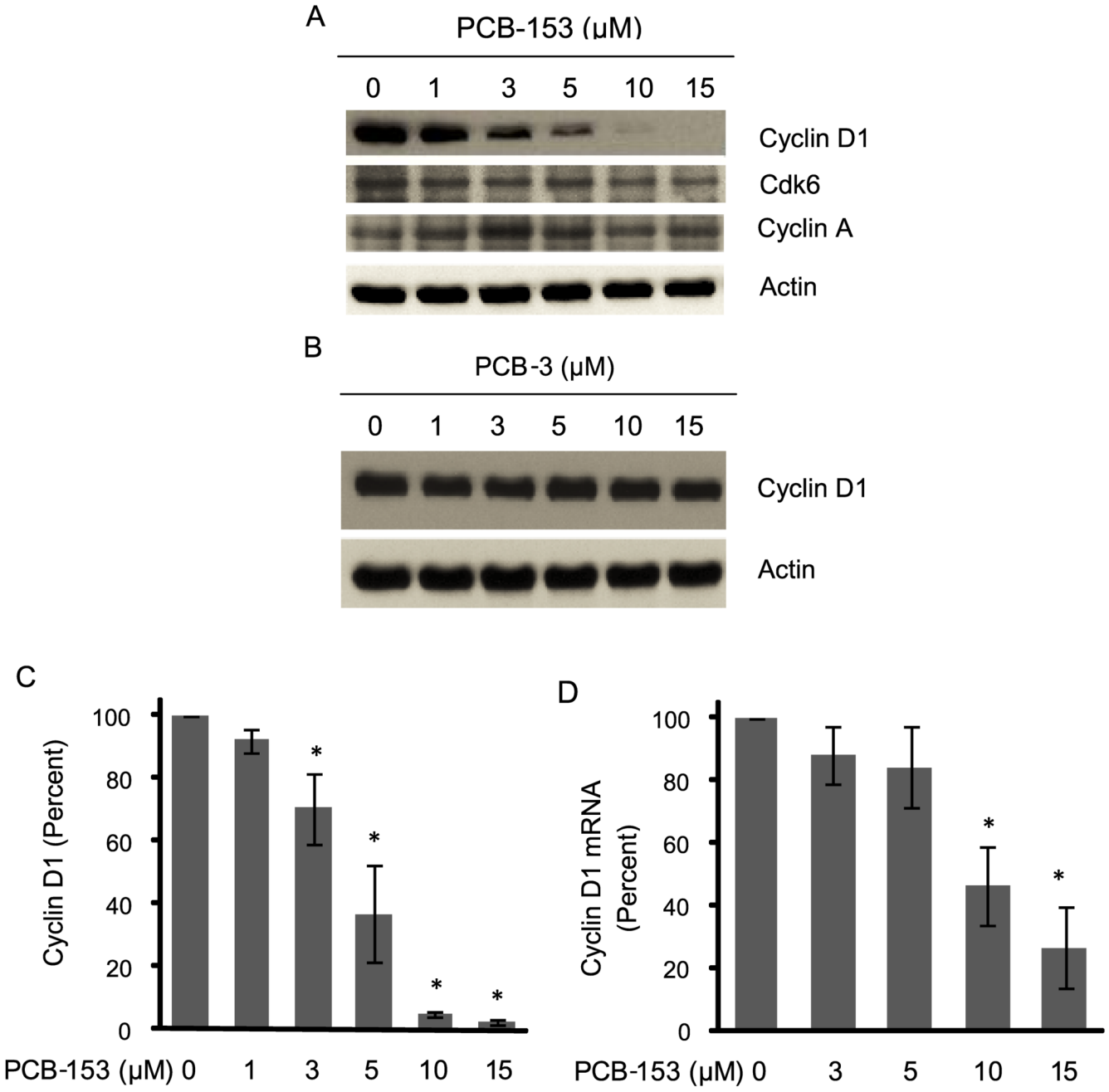

Fig. 2. PCB-153 treatments decreased cyclin D1 protein levels

MCF-10A cells were treated with 0–15 μM of **(A)** PCB-153 and **(B)** PCB-3 for 4 h, and harvested for immunoblotting analysis of cyclin D1 protein levels. Blots were reprobed with antibodies to cyclin A and actin. **(C)** Cyclin D1 fold-change was calculated first by normalizing to actin in individual samples and then relative to untreated control. Asterisks represent statistical significance compared to untreated control; n=3, $p < 0.05$. **(D)** Total cellular RNA was extracted at the end of 4 h of PCB-153 treatments, and cyclin D1 mRNA levels were measured using a quantitative RT-PCR assay; 18S rRNA levels were used as control for the assay. ANOVA followed by Tukey's *post hoc* test were used to assess statistical significance

of results. Asterisks represent significant difference between control and treated samples (n=3, $p < 0.05$).

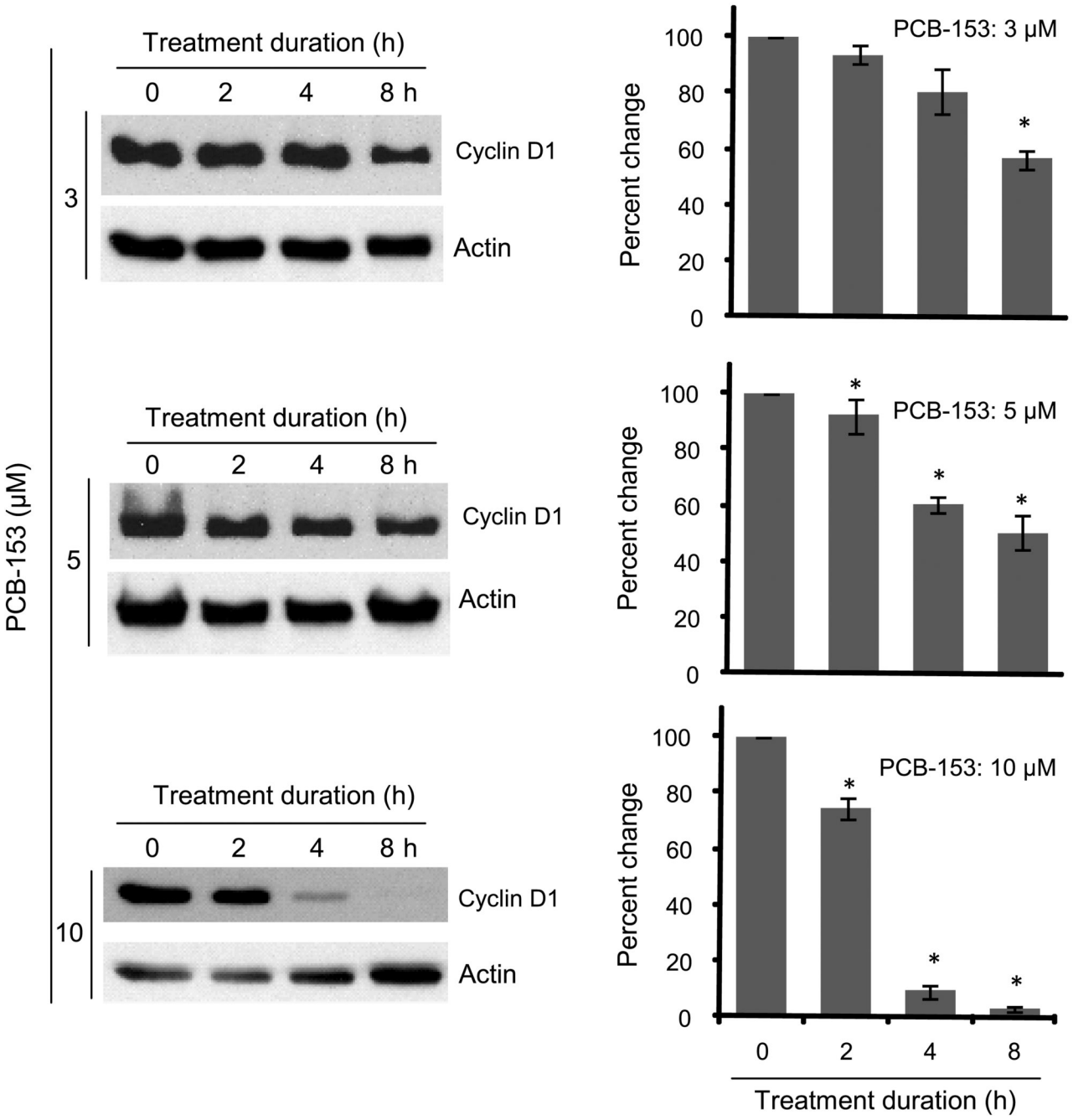

Fig. 3. Dose and duration dependent effects of PCB-153 on cyclin D1 protein levels

MCF-10A cells were treated with 3–15 μM of PCB-153 for 2–8 h. Cells were harvested at indicated times and analyzed for cyclin D1 and actin protein levels by immunoblotting. ANOVA followed by Tukey's *post hoc* test were used to assess statistical significance of results. Asterisks represent significant difference between control and treated samples (n=3, $p < 0.05$).

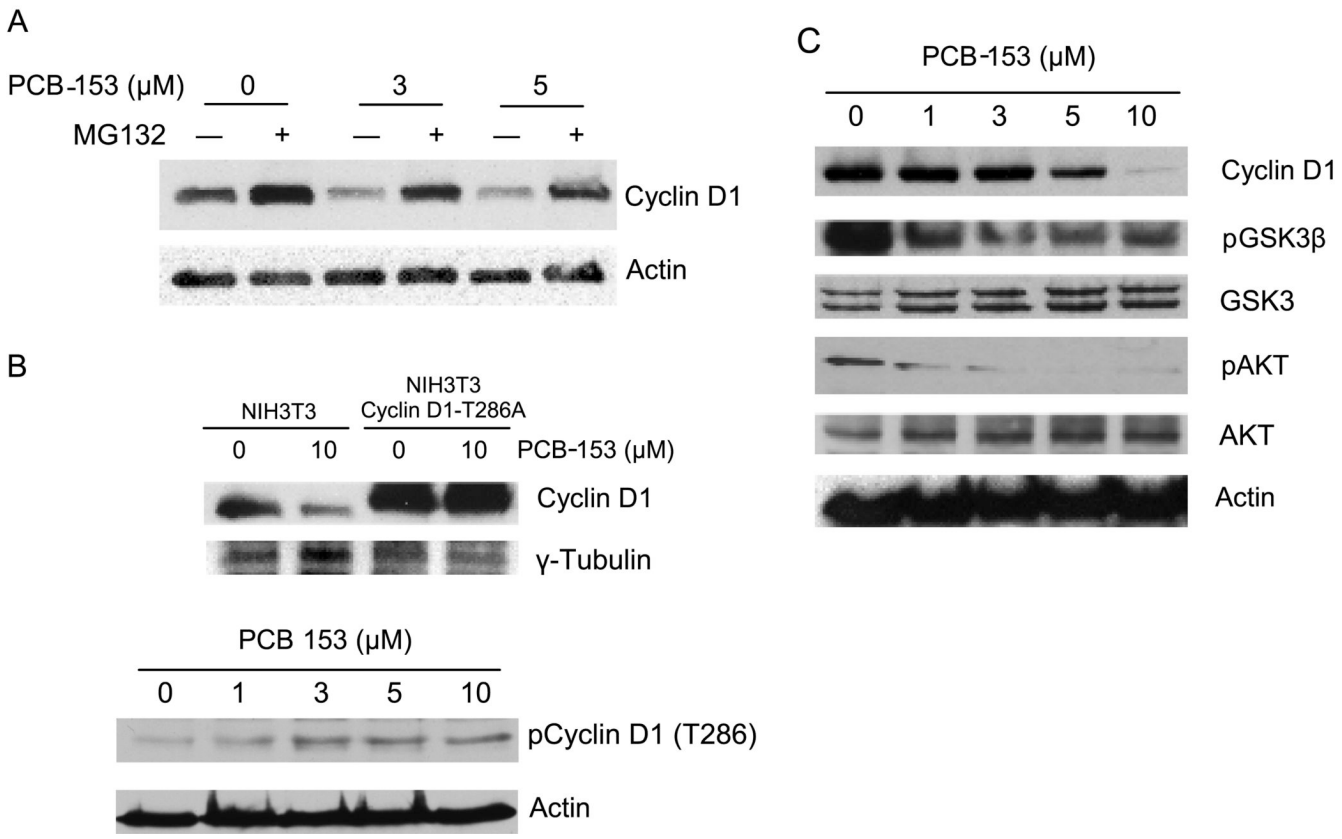

Fig. 4. Proteasome and T286 phosphorylation dependent pathways regulate cyclin D1 protein levels in PCB-153 treated cells

(A) MCF-10A cells were treated with 50 μM of MG132 for 45 min followed by addition of PCB-153 for 4 h. Cyclin D1 protein levels were analyzed by immunoblotting. **(B)** Upper-panel: NIH3T3 mouse fibroblasts carrying wild type and T286A mutant form of cyclin D1 were incubated with 10 μM PCB-153 for 4 h. Cyclin D1 protein levels were analyzed by immunoblotting; γ-tubulin levels were used for comparison. Two-way ANOVA followed by paired t test were used to compare the two groups of treatment; n=3, $p < 0.05$. Bottom-panel: MCF-10A cells were treated with different doses of PCB-153 for 4 h and harvested for immunoblotting analysis of the T286 phosphorylated form of cyclin D1; actin levels were used for comparison. **(C)** Immunoblot analysis of cyclin D1, phosphorylated AKT and GSK-3β, total AKT and GSK-3β, and actin.

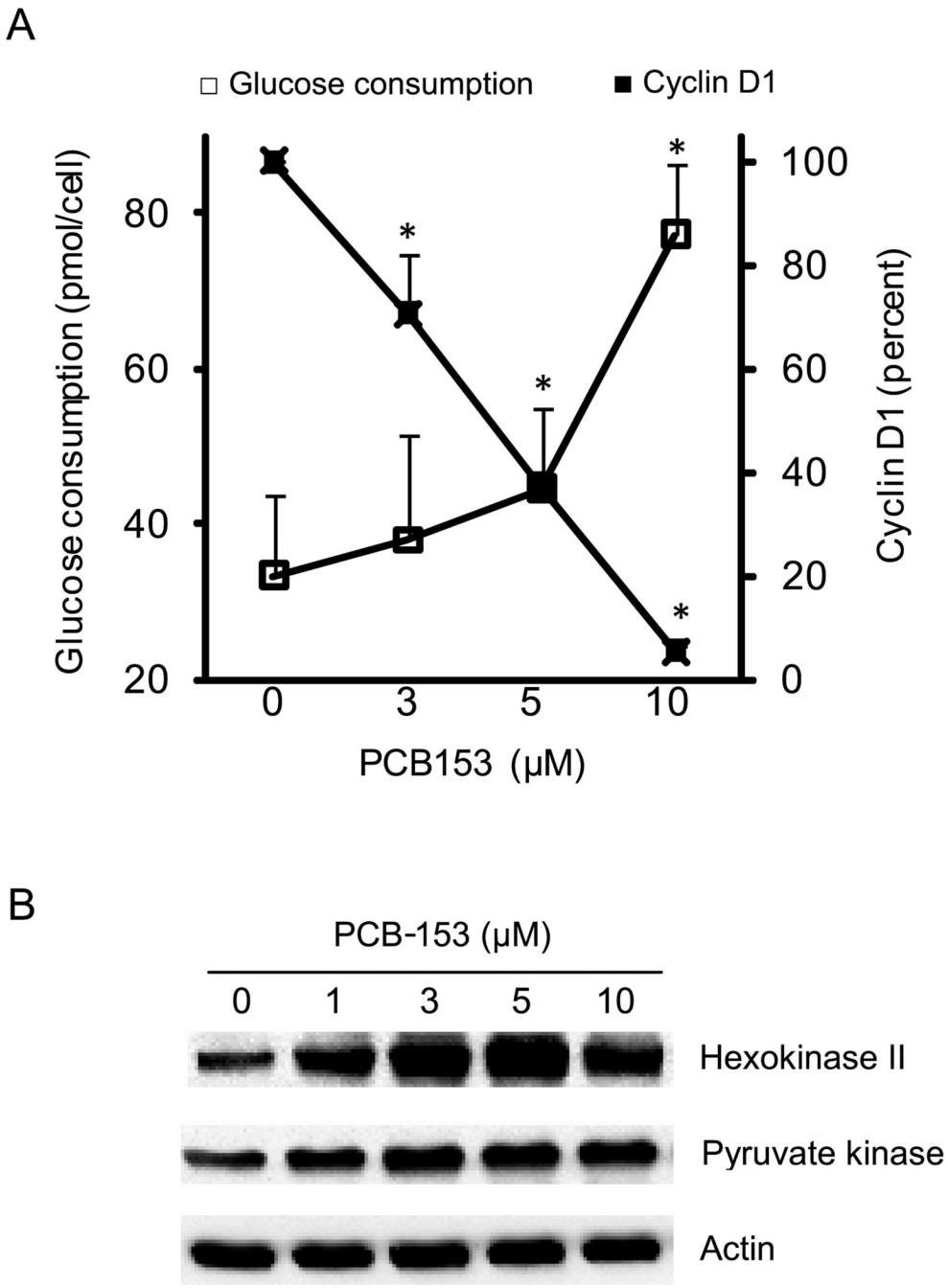

Fig. 5. PCB-153 induced decrease in cyclin D1 protein levels inversely correlates with cellular metabolism

(A) MCF-10A cells were incubated with PCB-153 for 8 h; medium was replaced with fresh medium and glucose consumption measured at the end of an additional 8 h. ANOVA followed by Tukey's *post hoc* test were used to assess statistical significance of results. Asterisks represent significant difference between control and treated samples ($p < 0.05$). **(B)** Immunoblot analysis of hexokinase II and pyruvate kinase protein levels; actin levels were used for comparison.